

# Cosmological experiments in liquid helium

P.C. Hendry and P.V.E. McClintock  
*Department of Physics, Lancaster University,  
Lancaster LA1 4YB, UK*

Fast passage through a continuous phase transition is expected to result in the creation of topological defects via the Kibble mechanism. Recent experiments involving the expansion of a small volume of liquid  $^4\text{He}$  through the lambda (superfluid) transition, as a model of the GUT (grand unified theory) symmetry-breaking transition of the early universe, are discussed and set in context. Copious creation of quantized vortices, analogous to cosmic strings, is expected but not observed. The possibility of developing a more sensitive version of the experiment is considered.

Key words: phase transition, early universe

PACS numbers: 05.70.F, 64.60, 64.70, 98.80.C

## 1. Introduction

There are just a few physical phenomena, predicted by theory, that would appear to lie forever beyond the reach of experiment. One of these is the symmetry-breaking phase transition that is believed to have occurred  $\sim 10^{-35}$  s after the dawn of time at the Big Bang. The energies involved are so large that it seems unlikely that this event can ever be reproduced and studied in the laboratory. This is unfortunate because, quite apart from its intrinsic interest, topological defects in space-time created during the transition are potentially of importance because they may perhaps have provided the primordial density inhomogeneities that later gave rise to galaxy formation.

Although the phenomenon itself is experimentally inaccessible, we can still hope to learn something about the underlying physics through studies of model systems that are described by equations of similar form. As we shall see, the cosmological phase transition is often treated with Ginzburg-Landau theory – using precisely the same approach as is used to describe 2nd order phase transitions in superconductors and superfluids. Thus we may anticipate that phenomena that arise in the latter, experimentally accessible, systems may have cosmo-

logical analogues and *vice versa*. In what follows, we describe in outline what is being learned about defect formation during the cosmological transition through experimental studies of the analogous transition in liquid  $^4\text{He}$ .

We start by introducing liquid  $^4\text{He}$  in Section 2, and we summarise the relevant properties of the superfluid phase, He II, in Section 3. In Section 4, we embark on what appears at first sight to be a completely separate subject and outline what is believed to have occurred just after the Big Bang, including the idea of the cosmological phase transition; and we then bring the two subjects together by showing that studies of liquid helium may be expected to illuminate analogous cosmological events. We discuss the experiments themselves in Section 5, and consider their interpretation in Section 6. Finally, in Section 7, we summarise the present status of such studies and draw interim conclusions.

## 2. Liquid helium

Helium enjoys the peculiar distinction of having been discovered in solar spectra by Janssen and by Lockyer long before it was found on earth by Sir William Ramsay. It proved to be extremely difficult to liquefy, frustrating Sir James Dewar but finally

succumbing only in 1908 to the large team assembled by Kammerlingh Onnes in Leiden [1]. Astonishingly, its superfluidity was overlooked for another three decades, but was then discovered independently and almost simultaneously (see e.g. [2, 3, 4]), in several different laboratories.

The reasons that helium is so hard to liquefy are two-fold. First, the He atom's inert gas structure means that the only inter-atomic attraction comes from the Van der Waals force, which is extremely weak. Secondly, the small atomic weight means that quantum mechanical zero-point energy is relatively very large. So the system reduces its free energy by expanding: liquid  $^4\text{He}$  has a density smaller by a factor of  $\sim 3$  than that expected for hard spheres of the appropriate radius and mass in contact with each other; in the case of the rare isotope  $^3\text{He}$ , which is lighter, the factor is  $\sim 4$ . So liquid helium, even in its normal (non-superfluid) state is in many ways rather gas-like because the atoms can easily slip past each other. Its viscosity, for example, is comparable with that of air at room temperature. The most important consequence of the large-amplitude zero point motion is that both isotopes of helium under its saturated vapour pressure remains liquid down to the lowest temperatures attainable, and they would still be liquid right down to the absolute zero of temperature. Pressures of about 25 and 35 atmospheres are needed to induce solidification, as illustrated in the phase diagram shown in Figure 1 (a) and (b) for  $^4\text{He}$  and  $^3\text{He}$  respectively.

Immediately following the discovery of superfluidity (see Section 3) London [5] proposed that these properties could be accounted for in terms of Bose-Einstein condensation (BEC), a phenomenon in which a significant fraction of the atoms condense (in momentum space) into the *same* quantum ground state. In an ideal gas, this fraction is expected to be unity at  $T = 0$ , but interactions in a system like helium (which, after all, is a liquid not a gas) should promote some of the atoms to “depletion levels”, thereby reducing the condensate fraction. Of course, BEC can occur only in a boson system (e.g.  $^4\text{He}$ ), for which there is no restriction on the occupancy of quantum states; but it can also occur in a fermion system (e.g. liquid  $^3\text{He}$ , electrons

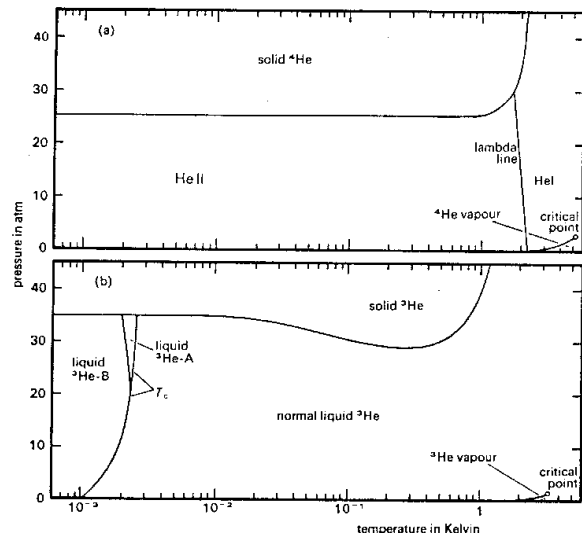


FIG. 1. Phase diagrams of (a)  $^4\text{He}$  and (b)  $^3\text{He}$ , after [10].

in a superconductor, white dwarf stars) if Cooper pairs with symmetric wavefunctions have formed, effectively creating bosons.

The existence of BEC in liquid  $^4\text{He}$  remained controversial, and was not established [6] until the 1980s. Ironically, although its superfluid properties are certainly associated in some way with BEC, superfluidity is *not* expected to occur in a Bose-condensed ideal gas. One very significant feature of BEC is the presence of a large number of atoms described by the same wavefunction, leading to London's idea of a macroscopic wavefunction describing the liquid. See [7] for a detailed discussion.

### 3. Superfluidity

Liquid helium exhibits a dramatic change in properties as it is cooled, passing through a phase transition at about 2K. It is known as the *lambda transition* because of the shape of the corresponding specific heat anomaly. In that it is continuous, with no associated specific heat, it can be considered to be a transition of second order. The properties are so different above and below the temperature  $T_\lambda$  of the transition that the liquid is referred to as He I and He II respectively in the two regimes: see Fig-

ure 1(a).

He II displays a whole range of bizarre and unexpected properties referred to collectively as superfluidity. It behaves as though it consisted of two separate but completely interpenetrating fluid components: a normal fluid component, much like any other liquid; and a superfluid component that exhibits the exotic properties. Their relative fractions are temperature dependent, with the normal fluid density  $\rho_n$  rising to 100% at  $T_\lambda$  and approaching zero at  $T = 0$ ; the fact that the superfluid fraction correspondingly approaches 100% at  $T = 0$  demonstrates immediately that it cannot be identified in a simple manner with the Bose condensate fraction, which is only  $\sim 10\%$  at  $T = 0$  on account of the interactions. It has been shown that the normal fluid component consists of the thermal excitations [8] of the liquid, phonons and rotons, moving in a “background” æther that corresponds to the superfluid component (see e.g. [9] or [10] for a discussion).

Examples of superfluid properties include a lack of viscosity, conferring the ability to flow easily through orifices of vanishingly small dimensions. Correspondingly, a small object moving through the liquid suffers no drag until a critical velocity is attained: the form of the drag–velocity measurements [11] shown in Figure 2 is typical, indicating zero drag until the Landau critical velocity [8] for roton creation has been exceeded. Another property that will be important for what follows is the ability of He II to support an unusual wave mode known as *second sound* in which the normal and superfluid components move in antiphase in just such a way as to keep the density constant. Whereas first (i.e. ordinary) sound is a pressure–density wave at almost constant temperature and entropy, second sound is a temperature–entropy wave at almost constant pressure and density. Its propagation velocity is far lower than that of first sound, being typically  $\sim 20 \text{ m s}^{-1}$  and falling to zero at  $T_\lambda$ .

The superfluid component cannot rotate, at least not in a conventional manner. Rather, the liquid in a rotating container either remains at rest relative to the fixed stars or, for faster rotations, becomes threaded with an array of quantized vortices [12] aligned parallel to the axis of rotation. Each

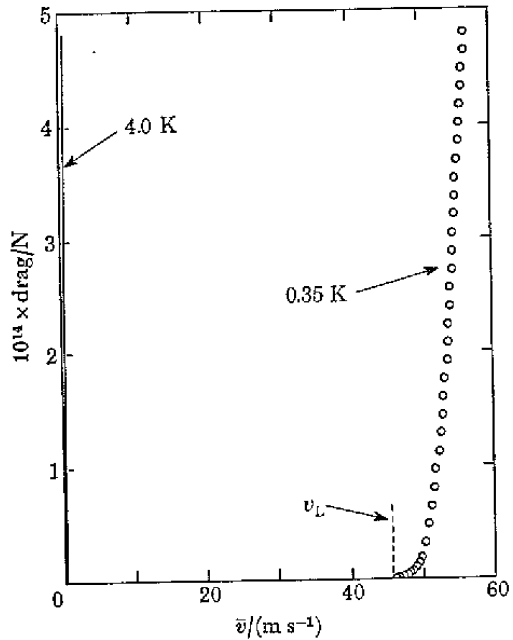


FIG. 2. The drag force on a small object (a negative ion) moving through liquid  $^4\text{He}$  measured (points) for a temperature well below  $T_\lambda$ : the drag is immeasurably small until the Landau critical velocity for roton creation  $v_L$  is exceeded. For comparison, the drag–velocity curve above  $T_\lambda$  is also shown by the full line near the ordinate axis. [11].

of these has a circulation equal to  $h/m_4$  where  $m_4$  is the  $^4\text{He}$  atomic mass, and a narrow core region of atomic dimensions: in effect, they are linear singularities where the superfluid wavefunction tends to zero, surrounded by superflow fields where the tangential velocity decreases as the reciprocal radius from the core. Vortices are not only produced by rotation. They are commonly created in the form of random tangles e.g. when flow velocities, or heat currents, exceed critical values. The creation mechanism at low temperatures seems to involve a form of macroscopic quantum tunnelling [13]; at the lambda transition, creation through an analogue of the Kibble mechanism (see below) is to be anticipated.

The cores of the vortices are “normal fluid component”, in that they can scatter excitations, whereas the surrounding flow field consists of superfluid.

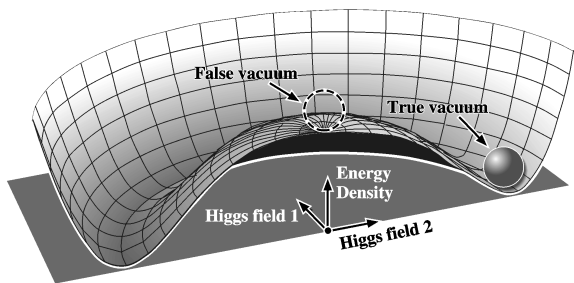


FIG. 3. Potential contribution to the free energy for the cosmological phase transition, after Guth and Steinhardt [18].

Thus vortices effectively couple the two fluids together. Consequently, second sound – involving counterflow of the two fluids – is strongly attenuated by the presence of vortices.

#### 4. The dawn of time

Astronomical observations have led to the widely accepted picture in which we exist within an expanding Universe: it seems that everything that we now see would have been together in a single point  $\sim 15 \times 10^9$  years ago. The universe is believed to have started in a hot Big Bang at that time, and to have been expanding since then. Calculations based on this general picture have been extremely successful in accounting for the cosmic microwave background radiation, the cosmic abundance of the elements, and many other features of the present Universe. Events at the earliest times are still shrouded in mystery, however, with a diversity of different theories either with or without inflation. For almost all cosmological theories, however, it is expected that the Universe will have undergone a series of symmetry-breaking phase transitions as it expanded and cooled.

There is an interesting analogy between liquid  $^4\text{He}$  and models of the early universe [14, 15, 16, 17]. It arises because both the lambda transition and the cosmological phase transition may be considered as being of second order, describable in terms of Ginzburg-Landau theory [7]. Thus, in each case, there is a potential contribution to the free energy

density of the form

$$V = \alpha|\psi|^2 + \frac{1}{2}\beta|\psi|^4 \quad (1)$$

where  $\psi$  is an order parameter. In the case of liquid  $^4\text{He}$ ,  $\psi$  is a complex scalar quantity representing the Bose condensate wave function; in cosmological models based on GUTs,  $\psi$  corresponds to Higgs fields. In each case,  $\beta$  is a constant and the parameter  $\alpha$  is temperature-dependent, being positive above the critical temperature  $T_c$  of the transition (which corresponds to the lambda transition  $T_\lambda$  in the case of liquid helium), and negative below it. At temperatures below the transition, therefore, the free energy in both cases takes on the same characteristic Mexican hat shape (Figure 3), whether plotted against the Higgs fields of the early universe, or against  $\text{Re}\psi$  and  $\text{Im}\psi$  in the case of  $^4\text{He}$ .

For  $T > T_c$ , the average value of  $\psi$  is zero, corresponding to the false vacuum or to He I. Below the transition, the symmetry is broken and  $\psi$  becomes finite, corresponding to the true vacuum or to He II. Below  $T_c$ , excitations of various kinds will exist at an equilibrium density that decreases very rapidly with growing  $(T_c - T)$ . In both cases, a fast passage through the phase transition to the broken symmetry state may be expected to yield topological defects, because of an event horizon that limits the size of causally connected regions and results in the order parameter of the nascent superfluid or true vacuum being spatially incoherent [19]. In the cosmological scenario, this process represents the Kibble mechanism [20] for creation of e.g. the cosmic strings (thin tubes of false vacuum) [21] that may have played an important role in seeding galaxy formation [22]. The analogue of cosmic strings, for liquid  $^4\text{He}$ , is quantized vortices [12].

The analogy between the cosmological and helium phase transitions may thus be summarised as follows –

Higgs field 1	$\longleftrightarrow$	$\text{Re } \psi$
Higgs field 2	$\longleftrightarrow$	$\text{Im } \psi$
False vacuum	$\longleftrightarrow$	He I
True vacuum	$\longleftrightarrow$	He II
Cosmic string	$\longleftrightarrow$	vortex line

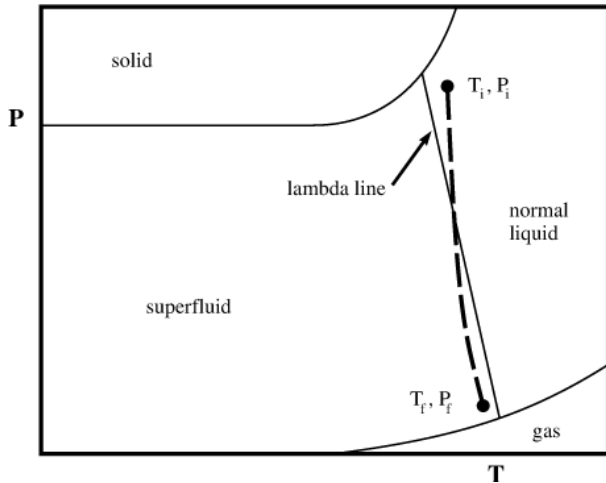


FIG. 4. Sketch of expansion trajectory through the  $^4\text{He}$  superfluid transition from a starting temperature and pressure  $(T_i, P_i)$  to final values  $(T_f, P_f)$ .

## 5. Cosmological experiments

If the above ideas are correct, a rapid passage of a sample of liquid  $^4\text{He}$  through the lambda transition would be expected to yield a large density of vortices. Remarkably, therefore, an investigation of this process, like the earlier studies of phase transitions in liquid crystals [23, 24], may be expected to yield information of cosmological significance.

The density of defects produced is expected [14, 15] to depend on the speed of the passage through the transition. Thus, to generate a large and easily measurable density of quantized vortices it is necessary to quench the liquid helium, from its normal He I state to its superfluid He II state, rapidly. This possibility seems at first sight to be precluded by the existence of a logarithmic infinity in the specific heat at  $T_\lambda$ , which would prevent rapid cooling of the liquid in the relevant temperature range; but Zurek [14, 15] pointed out that the pressure dependence of the lambda line  $T_\lambda(P)$  implies that the helium can instead be *expanded* through the transition, an operation that can be accomplished rapidly, e.g. along the dashed trajectory sketched in Figure 4.

An unexpected observation in the initial experiments [16] was that small densities of vortices were created even for expansions that occurred wholly

in the superfluid phase, provided that the starting point was very close to  $T_\lambda$ . The phenomenon was initially [17] attributed to vortices produced in thermal fluctuations within the critical regime, but it was pointed out [25] that effects of this kind are only to be expected for expansions starting within a few  $\mu\text{K}$  of the transition, i.e. much closer than the typical experimental value of a few mK. The most plausible interpretation – that the vortices in question were of conventional hydrodynamic origin, arising from nonidealities in the design of the expansion chamber – was disturbing, because expansions starting above  $T_\lambda$  traverse the same region. Thus some, at least, of the vortices seen in expansions through the transition were probably not attributable to the Zurek-Kibble mechanism as had been assumed. It was of particular importance, therefore, to undertake a new experiment with as many as possible of the nonidealities in the original design eliminated or minimised.

An ideal experiment would be designed so as to avoid all fluid flow parallel to surfaces during the expansion. This could in principle be accomplished by e.g. the radial expansion of a spherical volume, or the axial expansion of a cylinder with stretchy walls. In either of these cases, the expansion would cause no relative motion of fluid and walls in the direction parallel to the walls and presumably, therefore, no hydrodynamic production of vortices. The walls of the actual expansion chamber [16, 17] were made from bronze bellows, thus approximating the cylinder with stretchy walls. Although there must, of course, be some flow parallel to surfaces because of the convolutions, such effects are relatively small. It is believed that the significant nonidealities, in order of importance, arose from: (a) expansion of liquid from the filling capillary, which was closed by a needle valve 0.5 m away from the cell; (b) expansion from the shorter capillary connecting the cell to a Straty-Adams capacitive pressure gauge; (c) flow past the fixed yoke on which the second-sound transducers were mounted. In addition (d) there were complications caused by the expansion system bouncing against the mechanical stop at room temperature.

The current expansion cell, designed to avoid or

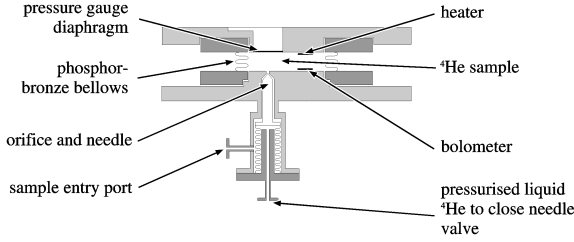


FIG. 5. The current expansion cell, designed so as to minimise hydrodynamic creation of vortices.

minimise these problems, is sketched in Figure 5. The main changes from the original design were as follows: (a) the sample filling capillary is now closed off at the cell itself, using a hydraulically-operated needle-valve; (b) the connecting tube to the pressure gauge has been eliminated by making its flexible diaphragm part of the chamber end-plate; (c) the second-sound transducers are also mounted flush with the end-plates of the cell, eliminating any support structure within the liquid; (d) some damping of the expansion was provided by the addition of a (light motor vehicle) hydraulic shock-absorber.

The operation of the expansion apparatus and the technique of data collection/analysis were much as described previously [16, 17], except that the rate at which the sample passed through the lambda transition was determined directly by simultaneous measurements of the position of the pull-rod (giving the volume of the cell, and hence its pressure) and the temperature of the cell. Distance from the transition was defined in terms of the parameter

$$\varepsilon = \frac{T_\lambda - T}{T_\lambda} \quad (2)$$

Thus the pressure-dependence of  $T_\lambda$ , and the non-constant expansion rate, were taken explicitly into account. Part of a trajectory recorded close to the transition during a typical expansion is shown in Figure 6. From such results, the quench time

$$\tau_Q = \frac{1}{\left(\frac{d\varepsilon}{dt}\right)_{\varepsilon=0}} \quad (3)$$

is easily determined. In the case illustrated, it was  $\tau_Q = 17 \pm 1.0$  ms. The position of the pull-rod is measured with a ferrite magnet attached to the rod,

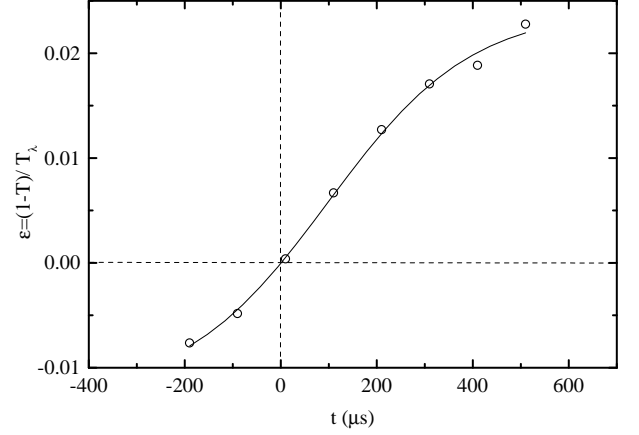


FIG. 6. Distance  $\varepsilon$  from  $T_\lambda$  versus time  $t$  for a typical quench. The reciprocal of the gradient at the transition gives the value of the ‘quench time’ parameter,  $\tau_q$  [33].

moving within a coil fixed to the cryostat top-plate. There is some evidence of a small time-lag between the expansion of the cell under the influence of the high-pressure liquid inside it, and the corresponding movement of the transducer. Thus the measured  $\tau_Q$  may tend to overestimate the quench time slightly.

Following an expansion though the transition, after  $T$ ,  $P$  and the velocity  $c_2$  of second sound have settled at constant values, a sequence of second-sound pulses is propagated through the liquid. If the anticipated tangle of vortices is present, the signal may be expected to grow towards its vortex-free value as the tangle decays and the attenuation decreases. Signal amplitudes measured just after two such expansions are shown by the data points of Figure 7. It is immediately evident that, unlike the results obtained from the original cell [16], there is now no evidence of any systematic growth of the signals with time or, correspondingly, for the creation of any vortices at the transition. One possible reason is that the density of vortices created is smaller than the theoretical estimates [14, 15, 26], but we must also consider the possibility that they are decaying faster than they can be measured: there is a “dead period” of about 50 ms after the mechanical shock of the expansion, during which the resultant vibrations cause the signals to be extremely noisy (which is why the error bars are large on early signals in Figure 7).

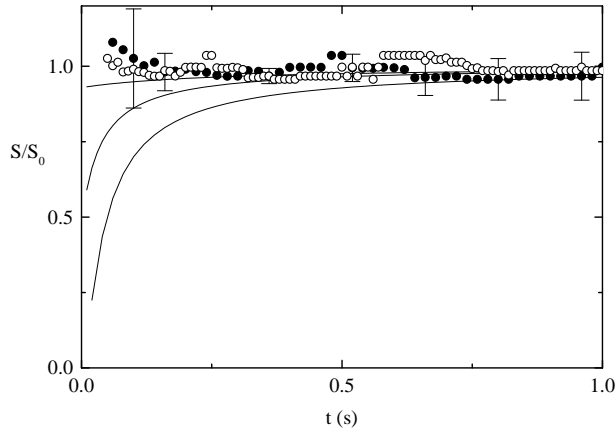


FIG. 7. Comparison of the measured evolution of the second sound amplitude (data points) with those calculated (curves) on the assumption of different initial vortex line densities  $L_i$  immediately after the expansion [33].

The rate at which a tangle of vortices decays in this temperature range is determined by the Vinen [27] equation

$$\frac{dL}{dt} = -\chi_2 \frac{\hbar}{m_4} L^2 \quad (4)$$

where  $L$  is the length of vortex line per unit volume,  $m_4$  is the  $^4\text{He}$  atomic mass and  $\chi_2$  is a dimensionless parameter. The relationship between vortex line density and second-sound attenuation is known [12] from experiments on rotating helium, and may for present purposes be written in the form

$$L = \frac{6c_2 \ln(S_0/S)}{B\kappa d} \quad (5)$$

where  $S_0$  and  $S$  are the signal amplitudes without and with vortices present,  $B$  is a temperature dependent parameter,  $\kappa = h/m_4$  is the quantum of circulation, and  $d$  is the transducer separation.

Integrating (4) and inserting (5), one finds immediately that the recovery of the signal should be of the form

$$\left[ \ln \left( \frac{S_0}{S} \right) \right]^{-1} = \frac{6c_2}{\kappa B d} \left( \chi_2 \frac{\kappa}{2\pi} t + L_i^{-1} \right) \quad (6)$$

Of the constants in (6), all are known except  $\chi_2$  and  $B$  which seem not to have been measured accurately within the temperature range of interest. We

therefore performed a subsidiary experiment, deliberately creating vortices by conventional means and then following their decay by measurements of the recovery of the second-sound signal amplitude. This was accomplished by leaving the needle-valve open, so that  $\sim 0.2 \text{ cm}^3$  of liquid from the dead volume outside the needle-valve actuator-bellows was forcibly squirted into the cell during an expansion. As expected, large densities of vortices were created. Plots of  $[\ln(S/S_0)]^{-1}$  as a function of  $t$  yielded straight lines [33] within experimental error in accordance with (6). By measurement of the gradient, and comparison with (6), for a number of such plots it was possible to determine  $\chi_2/B$  as a function of  $T$  and  $P$ . Fuller details will be given elsewhere, but it was found that  $\chi_2/B$  did not exhibit a strong temperature dependence and could be approximated by  $\chi_2/B = 0.004 \pm 0.001$  within the range of interest where  $0.02 < \varepsilon < 0.06$ .

The measured value of  $\chi_2/B$  was then used to calculate the evolution of  $S/S_0$  with time for different values of  $L_i$ , yielding the curves shown in Figure 7. From the  $\tau_Q$  measured from the gradient in Figure 6, and Zurek's estimate of

$$L_i = \frac{1.2 \times 10^{12}}{(\tau_Q/100 \text{ ms})^{2/3}} \quad [\text{m}^{-2}] \quad (7)$$

we are led to expect that  $L_i \approx 4 \times 10^{12} \text{ m}^{-2}$ . A comparison of the calculated curves and measured data in Figure 7 shows that this is plainly not the case. In fact, the data suggest that  $L_i$  is smaller than the expected value by at least two orders of magnitude.

Before discussing these results, we point out that there have also been two comparable experiments [30, 31] using liquid  $^3\text{He}$ , which also undergoes a superfluid transition when cooled to  $\sim 1 \text{ mK}$ , as indicated in Figure 1(b). Both experiments involve local heating of the liquid to above the superfluid transition by a nuclear reaction caused by neutron absorption, followed by an extremely fast temperature quench back into the superfluid phase. In one case [30] the production of vortices is inferred from an energy deficit; and in the other [31] the process is observed directly by growing the vortices to macroscopic dimensions in a rotating cryostat and detect-

ing them by nuclear magnetic resonance. In each of these experiments, it was reported that the density of vortices created was consistent with Zurek's theoretical predictions [14, 15, 26] based on the assumption of production via the Kibble mechanism.

## 6. Discussion

There are a number of comments to make on the null result obtained for liquid  $^4\text{He}$  (Figure 7) which, in the light of the apparently positive outcome from the earlier experiment [16], came as a considerable surprise. First, Zurek's estimates of  $L_i$  were never expected to be accurate to better than one, or perhaps two, orders of magnitude, and his more recent estimate [28] suggests somewhat lower defect densities. So it remains possible that his picture [14, 15, 26, 28] is correct in all essential details, and that the improved experiment with faster expansions now being planned (see below) will reveal evidence of the Kibble-Zurek mechanism in action in liquid  $^4\text{He}$ . Secondly, it must be borne in mind that (4), and the value of  $\chi/B$  measured from the experiment, refer to hydrodynamically generated vortex lines. Vorticity generated in the nonequilibrium phase transition may be significantly different, e.g. in respect of its loop-size distribution [29], may therefore decay faster, and might consequently be unobservable in the present experiments. Thirdly however, it is surprising that the  $^3\text{He}$  experiments [30, 31] (see above) appear to give good agreement with Zurek's original estimates [14, 15, 26] whereas the present experiment shows that they overestimate  $L_i$  by at least two orders of magnitude. It is not yet known why this should be, but a possible explanation of the apparent discrepancy has been proposed [32] by Karra and Rivers.

One way to provide a more sensitive test of the ideas underlying the Kibble/Zurek mechanism would be to repeat the experiment under conditions where the predicted initial vortex density  $L_i$  is larger: from (3),(2),(7) it is clear that the only way to increase  $L_i$  is to reduce  $\tau_Q$  by increasing the rate of expansion  $\left(\frac{d\varepsilon}{dt}\right)_{\varepsilon=0}$ . In principle one could consider a forced expansion, rather than allowing the

cell to expand under its own internal pressure as at present. Given the magnitudes of the forces involved (equivalent to 147 Kg weight for the present cell with  $P_i = 30$  bar), and the difficulties already being experienced with vibration after the expansion is abruptly halted, this option appears difficult. A better option must be to try to lighten all the moving parts so as to increase the acceleration for any given pressure.

In the present apparatus (Figure 5), most of the moving mass lies in the two disk-shaped compressor plates, a long pull-rod extending up to the cryostat top-plate at room temperature, and in the trigger mechanism. In a new cryostat, now being designed, we plan several radical changes to the expansion mechanism, as sketched in Figure 8. The disk-shaped plates will be replaced by the "spider-shaped" ones shown in Figure 8 (a). The trigger mechanism will be lightened as much as possible consistent with having the necessary strength, and placed on the top of the vacuum can flange in the main liquid  $^4\text{He}$  bath (Figure 8 (b). The stop will be placed immediately adjacent to it, thus eliminating most of the length of the long pull-rod from room temperature. A means of applying the large force (big vertical arrow) needed to compress the liquid will still be needed, of course, but could be provided by a chain or wire, or by a rod not bonded rigidly to the moving parts: it is needed only initially, to compress the liquid until the trigger latches, and can then be loosened. We calculate that, even without resort to special materials, these changes should reduce the mass of the moving components by  $\sim 80\%$ . From (7) this would imply an increase in  $L_i$  by a factor of  $\sim 3$ .

It is clear from the results of Figure 7 that it would be particularly advantageous if the noise on the signals at early time could be reduced. It is believed to result in large part from longitudinal vibrations in the pull rod, which is in tension. These vibrations result in small changes in the length – and therefore the pressure and temperature – of the sample, contributing a large noisy component to the second sound signals. Elimination of most of the length of the pull rod (Figure 8) should also,



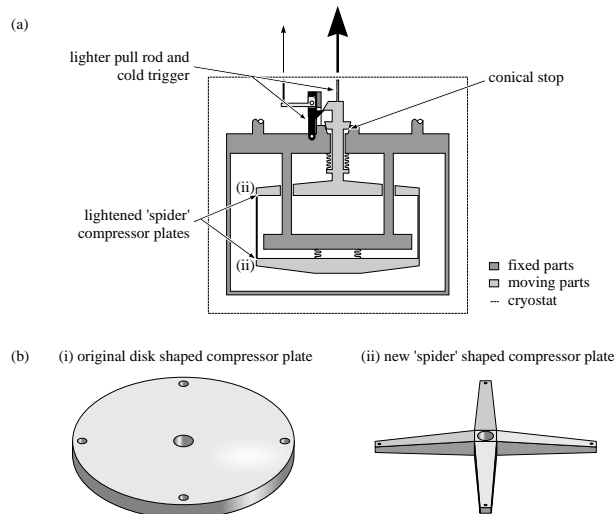


FIG. 8. Schematic diagram showing proposed modifications of the expansion mechanism (c.f. Fig. 1). (a) General view: trigger and stop are now in the main  $^4\text{He}$  bath; a rigidly attached pull-rod is no longer needed; and the stop is conical. (b) The two compressor plates are now “spider”-shaped. The cell is compressed between the fixed plate and the lower “spider”.

therefore, substantially reduce the effect probably also shifting it to higher frequencies where it will be easier to filter out.

A second way of reducing the shock at the end of the expansion, and thus the ensuing vibrations, is to replace the flat stop with a conical one (Figure 8). Most of the energy generated during the expansion will thus be dissipated by friction and dumped in the main liquid  $^4\text{He}$  bath. The optimal cone angle is yet to be determined, but it must obviously be made small enough to be dissimilar to the flat stop used earlier, but larger than that at which a cold weld might occur.

It is impossible to be quantitative about the extent to which noise at early time might be reduced by these changes, but a guess of a factor of 3–4 seems not unreasonable.

## 7. Conclusion

The present status of condensed matter cosmological experiments can therefore be summarised as follows. Studies based on fast, highly non-equilibrium,

temperature quenches through the  $^3\text{He}$  superfluid transition seem to demonstrate the Kibble mechanism in action, and they yield agreement with theoretical predictions of the initial vortex line density. Studies based on fast passage through weakly first-order phase transitions in liquid crystals also seem to yield results that are consistent with theory. But the  $^4\text{He}$  experiment, which in some ways provides the clearest and most direct approach, is in disagreement with theory by a factor of at least 100. This is disturbing because, while it is not difficult to think of ways in which additional vortices might be generated by small flow effects during the expansion process, it is difficult to find convincing reasons for a null result. Further experimental work on  $^4\text{He}$  is clearly needed.

It is concluded that, with some redesign, it should be not be too difficult to enhance considerably the sensitivity with which (7) can be tested, potentially enabling the lower bound on the disagreement between experiment and theory to be increased by an order of magnitude to  $\sim 10^3$ . Of course, if some vortex creation can be detected, it will then be necessary to test carefully whether it really arises via the Kibble mechanism or stems from conventional flow processes [16, 33, 34] caused by nonidealities during the expansion.

## Acknowledgement

We acknowledge valuable discussions or correspondence with S.N. Fisher, A.J. Gill, T. Kibble, R.A.M. Lee, R.J. Rivers, W.F. Vinen, G.A. Williams and W.H. Zurek. The work was supported by the Engineering and Physical Sciences Research Council (U.K.), the European Commission and the European Science Foundation.

## References

- [1] For an account of the early attempts to liquefy helium, see K Mendelssohn, *The Quest for Absolute Zero*, 2nd edn., Taylor and Francis, London, 1977
- [2] J F Allen and H Jones, *Nature* **141**, 243 (1938).
- [3] P L Kapitza, *J. Phys. (USSR)* **4**, 181 (1938).

- 
- [4] B V Rollin and F Simon, *Physica* **6**, 219 (1939).
- [5] F London, *Nature* **141**, 643 (1938).
- [6] V F Sears, E C Svensson, P Martel and A D B Woods, *Phys. Rev. Lett.* **49**, 279 (1982).
- [7] D R Tilley and J Tilley, *Superfluidity and Superconductivity*, 2nd edn, Hilger, Bristol, 1986.
- [8] L D Landau, *J. Phys. (USSR)* **5**, 71 (1941); and **11**, 91 (1947).
- [9] J Wilks, *The Properties of Liquid and Solid Helium*, Clarendon Press, Oxford, 1967.
- [10] P V E McClintock, D J Meredith and J K Wigmore, *Matter at Low Temperatures*, Blackie, Glasgow, 1984.
- [11] D R Allum, P V E McClintock, A Phillips and R M Bowley, *Phil. Trans. Roy. Soc. (Lond.) A* **284**, 179 (1977).
- [12] R J Donnelly, *Quantized Vortices in Helium II*, Cambridge University Press, 1991.
- [13] P C Hendry, N S Lawson, P V E McClintock, C D H Williams and R M Bowley, *Phys. Rev. Lett.* **60** 604 (1988).
- [14] W H Zurek, *Nature* **317**, 505 (1985).
- [15] W H Zurek, *Acta Physica Polonica B* **24**, 1301 (1993).
- [16] P C Hendry, N S Lawson, R A M Lee, P V E McClintock and C D H Williams, *Nature* **368**, 315 (1994).
- [17] P C Hendry, N S Lawson, R A M Lee, P V E McClintock and C D H Williams, *J. Low Temperature Phys.* **93**, 1059 (1993).
- [18] A Guth and P Steinhardt, “The inflationary universe”, in *The New Physics*, ed. P.C.W. Davies, Cambridge University Press, Cambridge, 1989.
- [19] A J Gill, *Contemporary Phys.* **39**, 13 (1998).
- [20] T W B Kibble, *J. Phys. A* **9**, 1387 (1976).
- [21] A Vilenkin and E P S Shellard, *Cosmic Strings and Other Topological Defects*, Cambridge University Press, Cambridge, 1994.
- [22] A Villenkin, *Phys. Rep.* **121**, 263 (1985).
- [23] I Chuang, R Durrer, N Turok and B Yurke, *Science* **251**, 1336 (1991).
- [24] M J Bowick, L Chandar, E A Schiff and A M Srivastava, *Science* **263**, 943 (1994).
- [25] W F Vinen, “Creation of quantized vortex rings at the  $\lambda$ -transition in liquid helium-4”, unpublished.
- [26] W H Zurek, *Phys. Rep.* **276**, 177 (1996).
- [27] W F Vinen, *Proc. R. Soc. Lond. A* **242**, 493 (1957).
- [28] P Laguna and W H Zurek, *Phys. Rev. Lett.* **78**, 2519 (1997).
- [29] G A Williams, *J. Low Temperature Phys.* **93**, 1079 (1993); *Phys. Rev. Lett.* **82**, 1201 (1999).
- [30] C Bäuerle, Y M Bunkov, S N Fisher, H Godfrin and G R Pickett, *Nature* **382**, 332 (1996).
- [31] V M H Ruutu, V B Eltsov, A J Gill, T W B Kibble, M Krusius, Y G Makhlin, B Placais, G E Volovik and W Xu, *Nature* **382**, 334 (1996).
- [32] G Karra and R J Rivers, *Phys. Rev. Lett.* **81**, 3707 (1998).
- [33] M E Dodd, P C Hendry, N S Lawson, P V E McClintock and C D H Williams, *Phys. Rev. Lett.* **81**, 3703 (1998).
- [34] M E Dodd, P C Hendry, N S Lawson, P V E McClintock and C D H Williams, *J. Low Temperature Phys.* **115**, 89 (1999).